Princeton Plasma Physics Laboratory
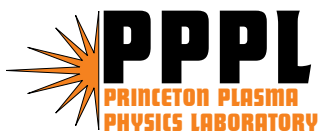
2-D Reflectometer Modeling for Optimizing the ITER Low-field Side Reflectometer System

G.J. Kramer, R. Nazikian, E.J. Valeo, R.V. Budny,
C. Kessel, and D. Johnson

September 2005

PPPL
PRINCETON PLASMA
PHYSICS LABORATORY

PPPL Report Disclaimers

Full Legal Disclaimer

Trademark Disclaimer

PPPL Report Availability

2-D reflectometer modeling for optimizing the ITER low-field side reflectometer system

G.J. Kramer,[*] R. Nazikian, E.J. Valeo, R.V. Budny, C. Kessel, and D. Johnson

Princeton Plasma Physics Laboratories,

P.O.box 451, Princeton, New Jersey 08543

(Dated: September 1, 2005)

Abstract

The response of a low-field side reflectometer system for ITER is simulated with a 2-D reflectometer code using a realistic plasma equilibrium. It is found that the reflected beam will often miss its launch point by as much as 40 cm and that a vertical array of receiving antennas is essential in order to observe a reflection on the low-field side of ITER.

---
[*]gkramer@pppl.gov

I. INTRODUCTION

Reflectometry is one of the key diagnostics for the International Thermonuclear Experimental Reactor (ITER) [1]. In the present design of ITER there are three major reflectometer systems envisioned: a low-field side system, a high-field side system and a plasma position control system. A fourth reflectometer system in the divertor has so far been deemed technically too difficult to construct [2]. Once a diagnostic is installed on ITER access to it is extremely difficult due to the very harsh enviroment and ITER's size. Removing a port plug in which the diagnostics are mounted for maintenance is an expensive and time consuming operation and has to be avoided as much as possible. A good analogy for ITER diagnostics are instruments mounted on satellites in space. Once the satellite is launched there is no access to the instrument to correct flaws. For ITER diagnostics something similar holds: once the the diagnostic is launched in ITER-space (mounted on ITER) one normally does not have access to it any more for repairs and/or changes. Thus in the design phase of diagnostics for ITER it is of paramount importance to study and predict its response in relation to expected plasma scenarios in order to optimize the diagnostic and find possible weaknesses and correct them before building the diagnostics.

In this paper we study the behavior of the low-field side reflectometer system with a full wave 2-D reflectometer code, FWR2D [3]. The FWR2D code has been validated successfully against laboratory experiments [4, 5] and it has been applied to interpret reflectometer data that was taken on the JT-60U tokamak [6].

After discussing the used ITER target plasma in section II we study the relativistic effects due to the finite electron temperature on the reflection layers in section III. Reflectometer simulations are presented in section IV and based on those results an antenna system for the ITER low-field side reflectometer system is proposed in section V. This is followed by the conclusions in section VI.

II. ITER TARGET PLASMA

Various tools are being used for integrated modeling of ITER plasmas, including the rampup to steady conditions and rampdown to termination. One set of tools is a combination of the Tokamak Simulation Code (TSC) [7] with the GLF23 model [8] to predict the
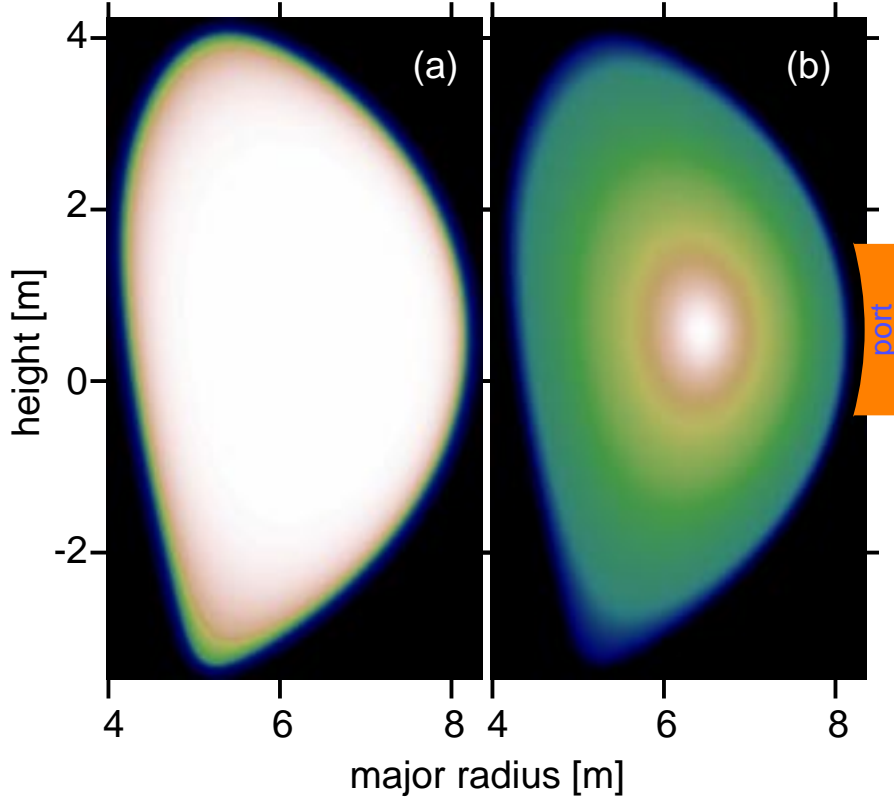
FIG. 1: color contour plot of (a) the electron density and (b) the electron temperature of the ITER plasma used in this paper. The maximum density, indicated in pink, is $6 \ 10^{19} m^{-3}$ and the maximum temperature is 26.5 keV.

temperature evolution, and the TRANSP code [9] with detailed heating and current drive capabilities. ITER plasma regimes that have been modeled this way include amongst others the ELMy H-mode and the Hybrid regime. The Hybrid regime has a higher confinement than the ELMy H-mode and typically a magnetic safety factor at the plasma center that is larger than one. In the reflectometer simulations that follow we have used a Hybrid plasma at a time when the current has reached its flat top value of 15 MA and the density is still rising slowly. A cross section of the plasma with electron density and temperature contours is shown in fig. 1. The plasma shape of ITER is up-down assymetric due to the divertor and as a consequence the flux surfaces at the mid-plane are in general not vertical but tilted slightly. in section IV we investigate the effects of this tilt on low field side reflectometry. The electron density profile is flat in the core with steep density gradients at the edge (see fig. 2a). The edge region with the density gradients can only be probed with O-mode reflec-

3
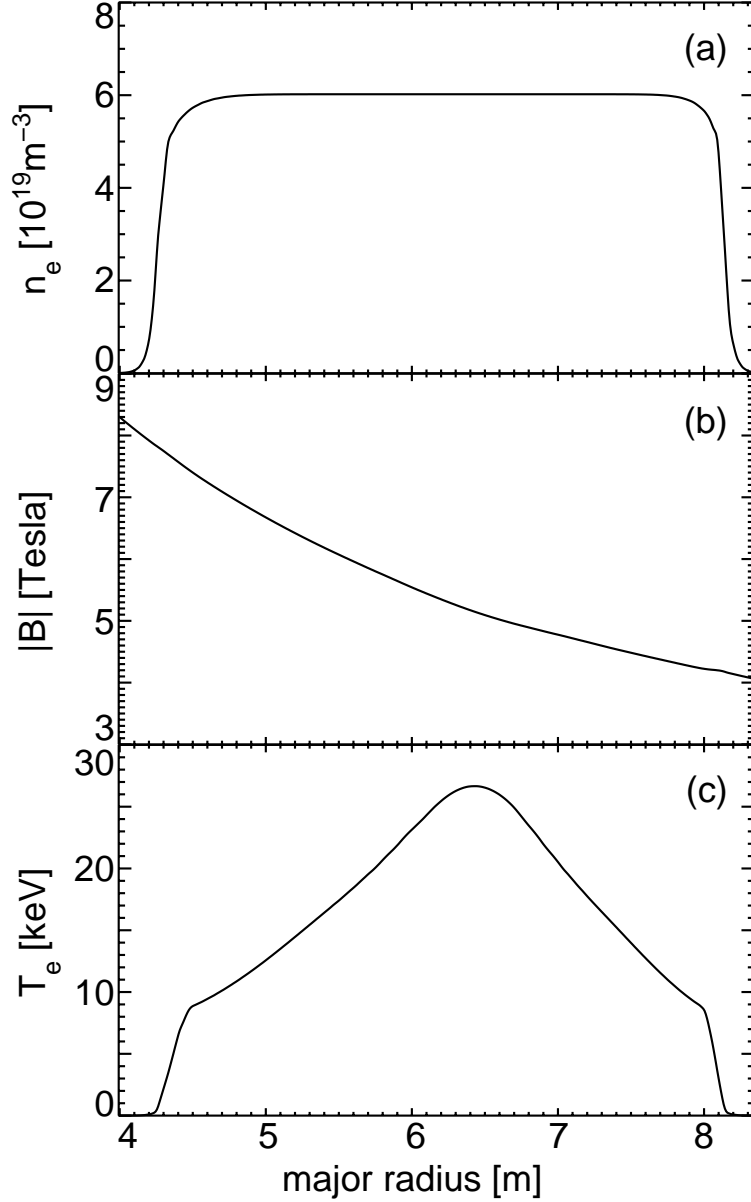
FIG. 2: The electron density (a), magnetic field (b), and electron temperature (c) at the plasma mid-plane.

tometry. In this paper we aim to study the reflectometer response from different parts of the plasma, not only the edge, therefore we have performed our simulations using the upper X-mode reflection layer. The modulus of the magnetic field, which enters in the equation for the X-mode reflection layers has an approximate $1/R$ (R the plasma major radius) dependence (fig. 2b) and therefore it is expected that most parts of the plasma are accessible from the low field side with upper X-mode reflectometry for sufficiently low densities.

III.   ELECTRON TEMPERATURE EFFECTS

The electron temperature which is shown in figs. 1b and 2c is high, up to 26.5 keV, and peaked at the plasma center. This has two effects on the operation of microwave reflectometry: i) relativistic corrections to the plasma permitivity become important and ii) microwaves can get adsorbed by the relativistically down-shifted second harmonic Electron Cyclotron Emission (ECE) layer. For the design of the reflectometer system this attenuation can make it difficult to get sufficiently strong reflected signal back from layers beyond the hot core but this does not affect the wave propagation in the plasma as calculated with the present 2-D code. The calculation of absolute power levels is a true 3-D problem and is not addressed in this paper.

In the cold plasma approximation the plasma permitivity is only a function of the electron density and the magnetic field strength. In fusion plasmas, however, relativistic effects due to the electron thermal velocity modify the plasma permitivity [10]. For plasmas in ITER where central electron temperatures are expected in the order of 15 to 30 keV relativistic corrections significantly modify the location of the reflection layers. The upper X-mode reflection layer is affected more strongly than the lower X-mode and O-mode reflection layers [11].

We have calculated the upper X-mode reflection contours using the cold plasma approximation (fig. 3a) and using a relativistic expression which takes into account the finite electron temperature (fig. 3b). In these relativistic calculations we have used an effective electron mass, m_e^*, given in [12] as:

$$\frac{m_e^*}{m_e} = 3K_2(\mu)/\mu^2 \int_0^\infty \frac{p^4 \exp(-\mu\gamma)}{\gamma(\gamma - s\Omega)} \mathrm{d}p \tag{1}$$

with m_e the electron rest mass, p the electron momentum, $\mu = m_e c^2/T_e$, T_e the electron temperature, $K_2(\mu)$ the modified Bessel function of the second kind, $\gamma = \sqrt{1 + p^2}$, $\Omega = \omega_c/\omega_s$ the electron cyclotron frequency divided by the cut off frequency and $s = 1, 0, -1$ for the upper X-mode, O-mode, and lower X-mode cut off layer, respectively.

Because of the nearly constant density and the dominant $1/R$ dependence of the magnetic field, the upper X-mode reflection layers form nice parallel mirrors if electron temperature corrections are neglected (fig. 3a) and the reflected signals return back to the launch point. When electron temperature corrections are included, the reflection layers curve strongly
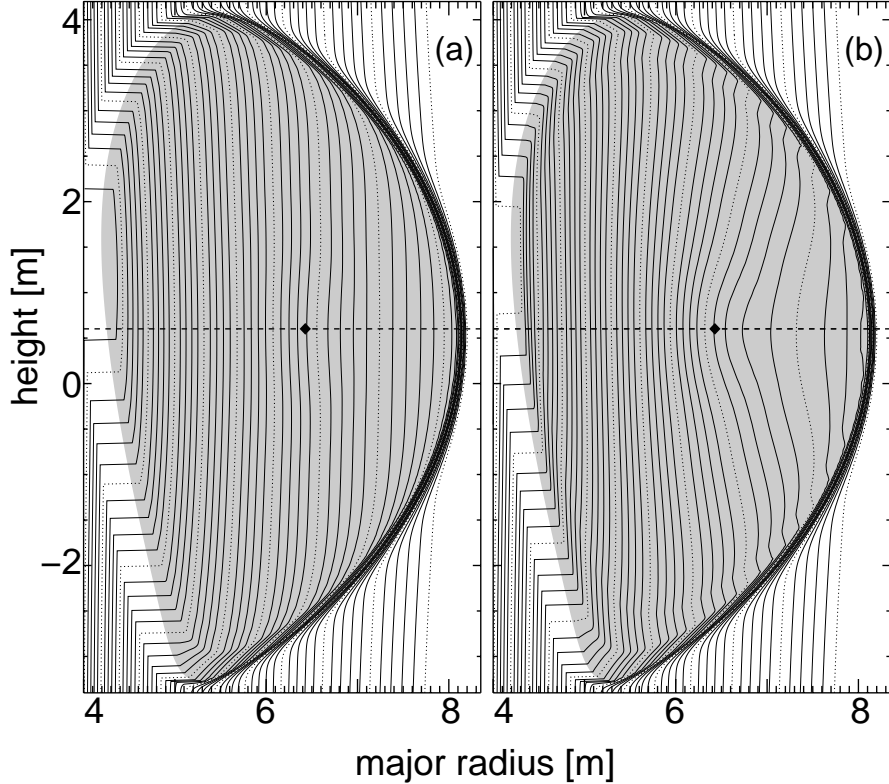
FIG. 3: Upper X-mode contours for a cold plasma ($T_e = 0$) (a) and for a hot plasma (b). The contours range from 120 GHz at the right in steps of 2 GHz while multiples of 10 GHz are indicated with dotted lines. The contour at the left is 232 GHz and 230 GHz for (a) and (b) respectively. The contour that passes through the plasma center (indicated with a diamond) is 172 GHz in (a) and 158 GHz in (b).

(fig. 3b) due to the peaked electron temperature profile. The returning waves are generally reflected to a location away from the transmitter antenna. In the next section we investigate where the reflected signals return to from these curved reflection layers.

IV. REFLECTOMETER SIMULATIONS

For proper operation of a reflectometer system it is crucial that the reflected waves arrive at the receiver antenna. therefore, it is important to understand how the microwave beam is influenced by the plasma through which it propagates and how it is reflected from a curved and/or tilted reflection layer. Electron density, temperature, and magnetic field
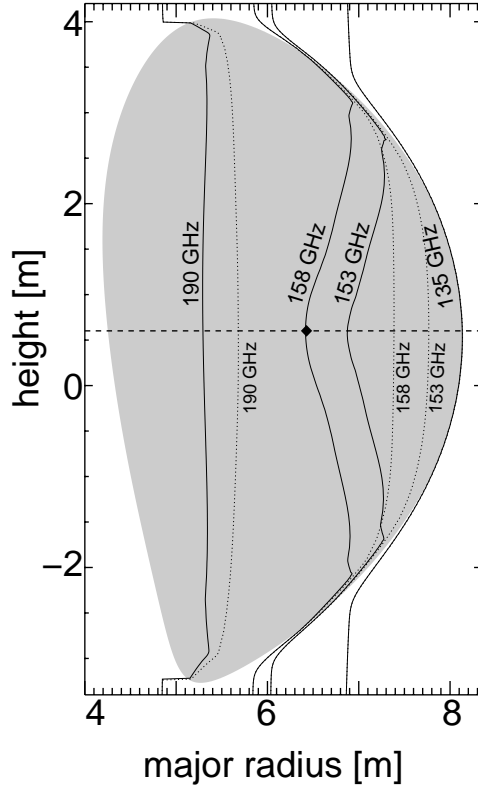
FIG. 4: Upper X-mode contours for the selected frequencies that are studied in detail.

gradients in the plasma can refract the microwave beam in such a way that the reflected beam does not come back to the receiver antenna which is conventionally located close to the launching antenna. The alignment between the reflection layer and the microwave beam is also very important, especially when the distance between the reflection layer and the receiving antennas is large as is the case for ITER. A small misalignment already steers the reflected beam away from the receiving antenna and the signal is lost.

We have studied the effect of the curved flux surfaces for four selected frequencies, 135, 153, 158, and 190 GHz. The reflection layers for those frequencies are shown in figure 4. The 135 GHz reflection layer is very close to the low-field side edge, it is convex, and relativistic corrections are negiglible because of the low edge electron temperature. After taking into account the relativistic corrections, the 153 and 158 GHz reflection layers become concave near the mid-plane, and they shift inward by 0.89 and 0.97 m at the height of the transmitter antenna, respectively, compared to the cold plasma reflection layers. The 190 GHz reflection layer shifts inward by 0.39 m and becomes slightly concave due to the relativistic effects.

In present-day experiments the shape of the reflection layer is usually convex due to a non-zero density gradient and "low" electron temperatures. Reflection from a convex reflection layer leads to a defocusing of the microwave beam and the reflected power is spread over significant range on the detector plane. (An example of such a conventional reflection is shown in fig. 1 of ref. [6]). In ITER, however, with its flat density profile and high and peaked electron temperature, the upper X-mode reflection layers are concave at the mid-plane over a lare frequency range as shown in figure 3b. These concave reflection layers lead to a focusing of the reflected beam and also affect the spread of the microwave power as discussed next.

For the study of the focusing and alignment properties of the reflection layers we have performed simulations with the following parameters. For the four selected frequencies we have taken a Gaussian beam with a full width half maximum (FWHM) for the power of 9 cm and without beam divergence. The latter was taken in order to see clearly the (de)focusing effect due to the reflection layer in the plasma. The transmitter and receiver antennas were located at R=9.0 m which is 0.85 m away from last closed flux surface. We have moved our transmitter antenna from 10 cm below to 10 cm above the plasma mid-plane which is at 59.26 cm, in steps of 1 cm and recorded the reflected signal at the detector plane. Even though the 2-D code that was used is very fast, each calculation took between 3 minutes and 10 hours of CPU time on a 2.4 GHz AMD Opteron dual processor machine with 16 Gb of memory running Redhat Linux. The long CPU times were due to the large computational domains used in some of simulations which were dictated by the large size of ITER and the curvature of the reflection layers.

Results of our simulations are shown in fig. 5 where we have plotted the location of the maximum reflected signal, and the corresponding -3 dB points as a function of the transmitter location. The center of the receiver antenna for the case when the receiver antenna is mounted next to the the transmitter antenna as is currently proposed for the ITER low-field side reflectometer system is indicated as a dashed line in fig. 5.

From fig. 5a it can be seen that for the edge-localized reflection with a frequency of 135 GHz the reflected signal returns back to the transmitter location and the FWHM has increased from 9 to 14 cm, showing the defocusing due to the convex reflection layer.

The reflection of 153 GHz from a concave reflection layer shows some interesting features (fig. 5b). When the waves are launched below the mid-plane the reflected beam at the
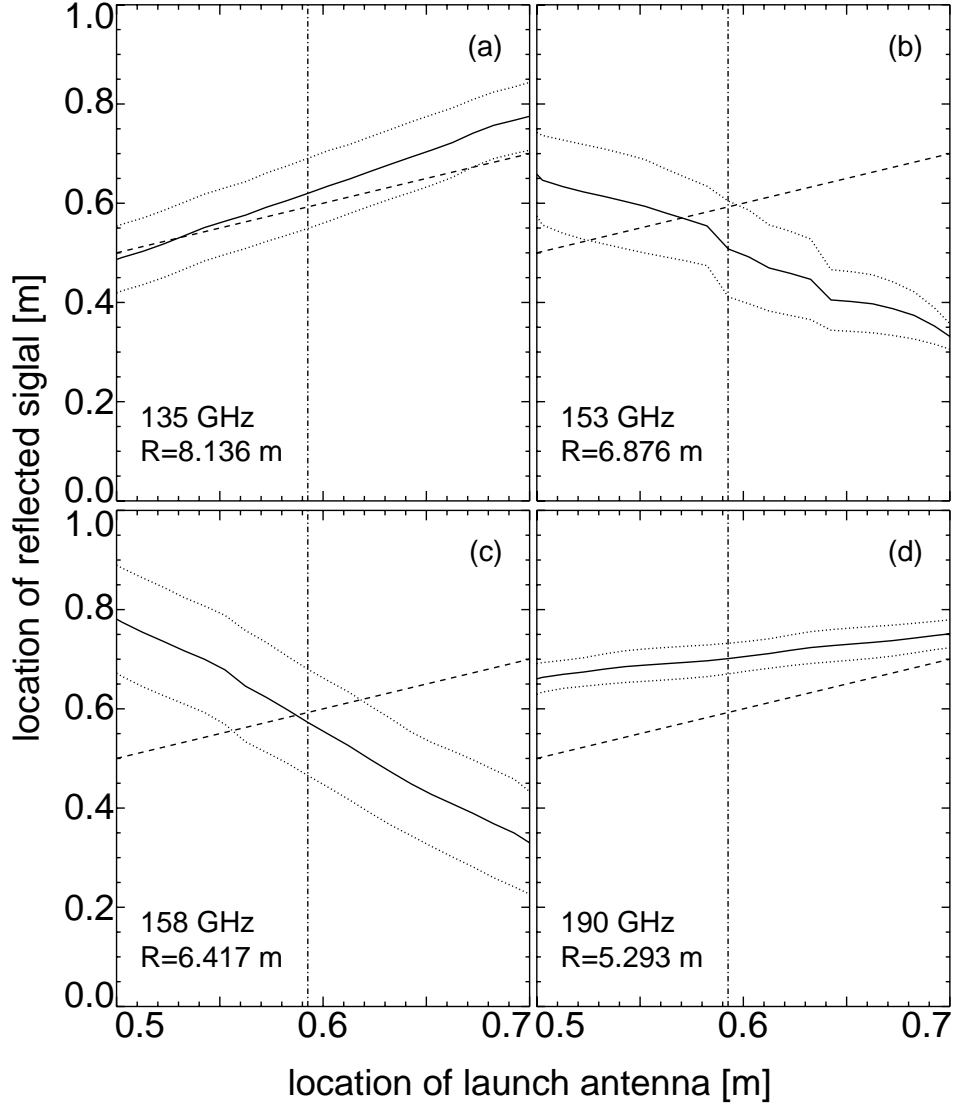
FIG. 5: Location of the maximum (solid line) reflected signal as a function of the position of the launch antenna for (a) 135 GHz, (b) 153 GHz, (c) 158 GHz, and (d) 190 GHz. At the dotted lines the signal has decreased to 50% and the dashed line indicate the center of the receiver antenna for the case when the receiver antenna is mounted next to the the transmitter antenna. The vertical dash-dotted lines indicate the plasma mid-plane.

detector plane has spread to 19 cm FWHM while launching the waves 10 cm above the mid-plane the FWHM has decreased to less than 5 cm. The concave curvature of the reflection layer focuses the reflected waves in the plasma. Moving along the reflecting surface from 10 cm below to 10 cm above the mid-plane changes the focus from 30 cm to 120 cm in

FIG. 6: The square root of the electrical field power for the 158 GHz full-wave solution at the cut-off (left) and the focus that is formed due to the concave curvature of the reflection layer. The intensity from low to high is indicated from black, blue, green, yellow, to white.
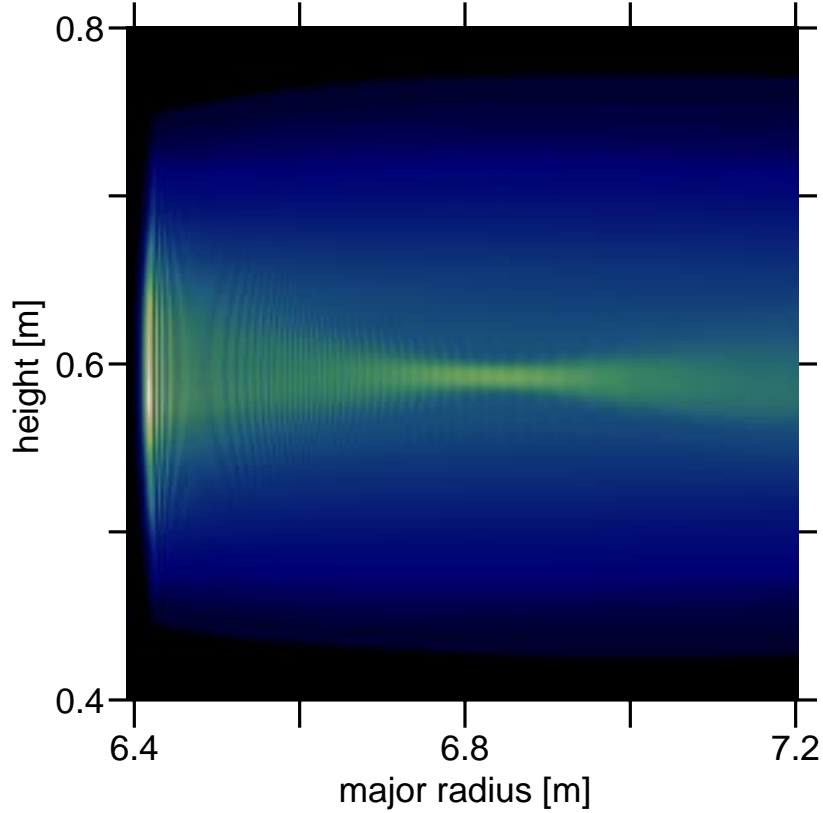
front of the reflection layer and hence the spread of the reflected signal at the detector plane decreases. Not only the width of the reflected beam changes with launch position but also the location of the maximum signal as can be seen in fig. 5b. This is due to a small tilt of reflection layer. A receiver antenna that is mounted next to the transmitter antenna will not detect the reflected signal when the transmitter-receiver antenna pair is away from the plasma mid-plane.

The vertical range over which a reflected signal returns to the launch location is even smaller for the 158 GHz channel (fig. 5c). The reflection of 158 GHz comes from a layer that is located 1 cm beyond the plasma center. The FWHM of the reflected 158 GHz beam is 22 cm and it is independent of the vertical position, indicating that the curvature of this reflecting layer is constant. The 158 GHz reflected beam has a focus in the plasma which is located 44 cm in front of the reflection layer as can be seen in fig. 6.

Because the ITER plasma shape is not up-down symmetrical due to the lower X-point at the divertor, the reflection layers at the high-field side are tilted slightly with respect to the vertical. This steers the reflected 190 GHz beam well away from its launch point as can be seen in fig. 5d. The curvature at the 190 GHz layer is such that the FWHM of the reflected beam is reduced to 6 cm from the initial 9 cm at the launch antenna.

From the simulations presented above it is clear that the alignment of the reflectometer system with the plasma mid-plane is very important for detecting the reflected signals, especially for reflections deeper in the plasma and away from the low-field side edge. It is expected that the plasma mid-plane in ITER is not fixed but it will vary with different plasma scenarios. The design for the low-field side reflectometer system needs to have enough build-in flexibility to cope with reflected signals that do not return to their launch point. In the next section we discuss some of the techniques to obtain such a flexibility.

V.   ANTENNA SYSTEM

In the simulations so far we have used a parallel microwave beam without any divergence. This beam was chosen to clearly see the effects of the reflection layer curvature and reflection layer angle on the returned signals. One way to broaden the reflected wave distribution at the antenna plane is to launch a divergent microwave beam. In this way some of the power can return to the location of the receiver antenna. The effect of spreading the incident beam, launched at the plasma mid-plane, on the width of the reflected beam is shown in fig. 7 for 135, 158, and 190 GHz. From this figure it can be seen that making a divergent beam spreads the reflected power over a much wider area on the detector plane, especially for the frequencies that probe the plasma core.

The disadvantage of spreading the reflected beam power over a wider area is that the reflected power that is detected with the receiver antenna approaches the noise background. Even if the launched microwave beam has a significant spread there are plasma scenarios possible with the plasma mid-plane displaced well above or below the plane defined by the reflectometer. In those cases the reflected signals still miss the receiver antenna even though the incident beam has a significant spread.

A second option to make the reflected signal return to a receiver antenna situated next to the transmiter antenna is by using steerable antennas. There are two good reasons to
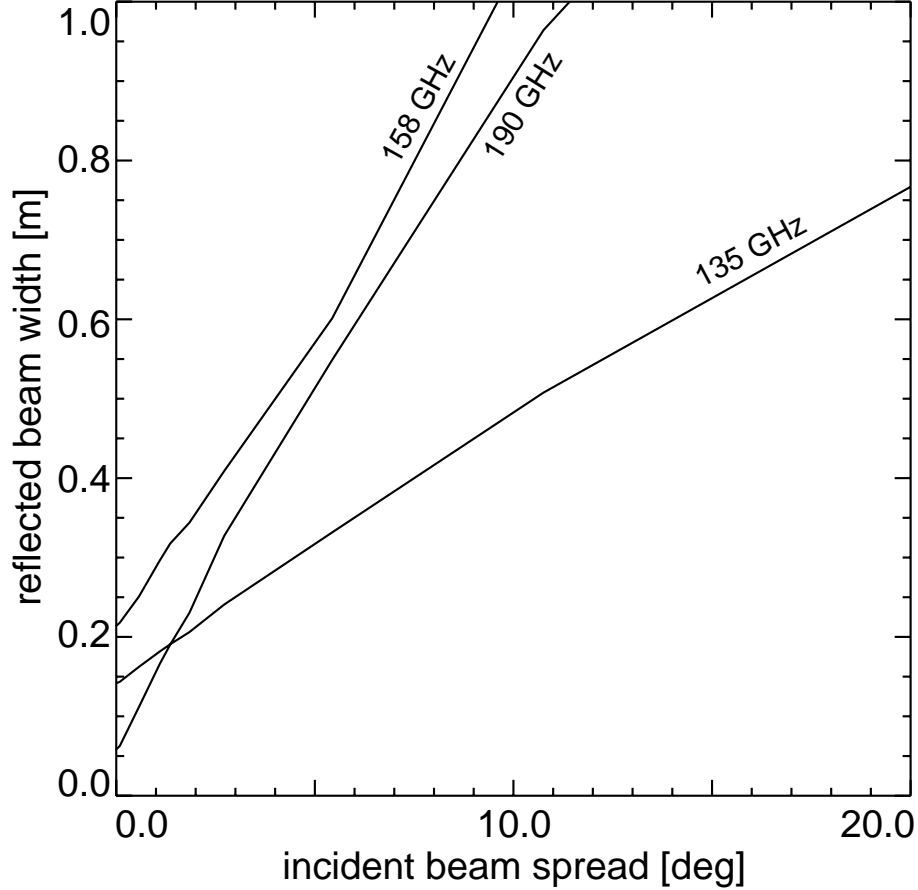
11

FIG. 7: The reflected beam width, defined as the distance between the -3 dB contours left and right from the maximum reflected power, as function of the incident spread, defined as the angle between the -3 dB contours left and right from the maximum incident power, for 135, 158, and 190 GHz microwave beams launched at the plasma mid-plane.

reject this idea. First, it complicates the hardware inside the port plug close to the plasma by introducing moving parts. Second, it might not be possible to steer the antennas to such a position that all the launched frequencies return to the receiver antenna.

A third option to detect reflected signals is to use a vertical array of receiver antennas. Antennas can be very robustly built, mounted near the plasma and the microwave signals can be transported without problems to a region behind the biological shield where they can be detected and processed seperately for each receiver antenna. With an array of receiver antennas it is quite possible to detect the reflection from all the launched frequencies under most plasma shapes and conditions. The drawbacks, however, are that each receiver antenna
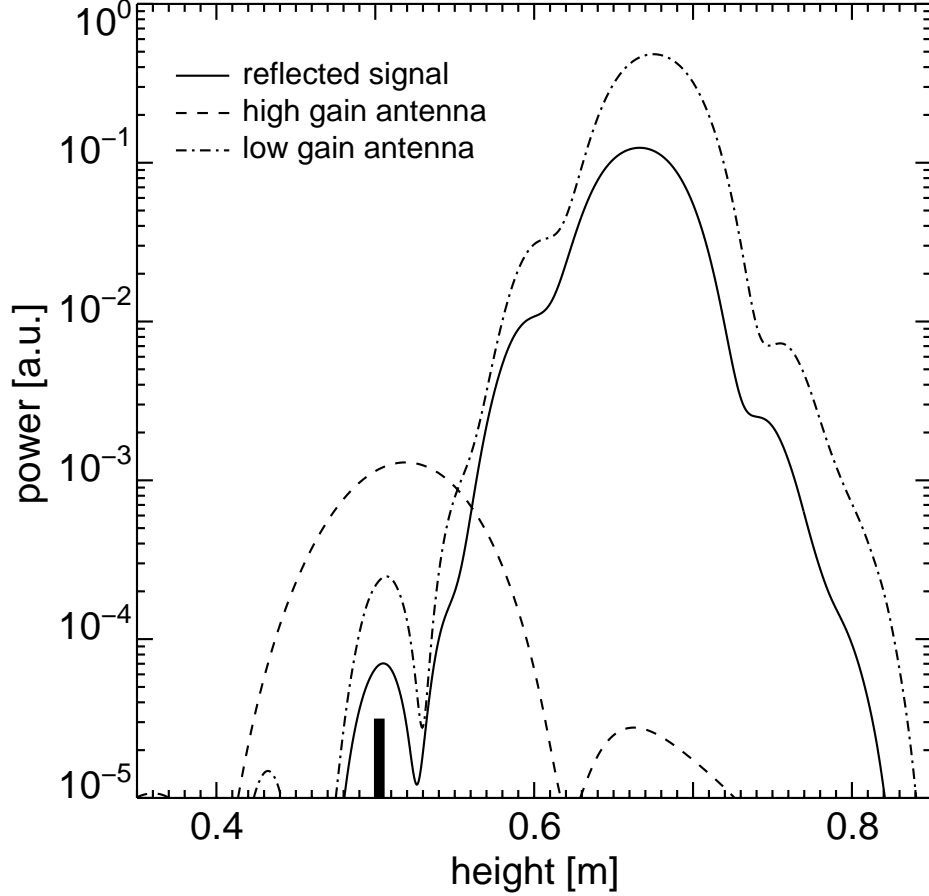
FIG. 8: The power of the 190 GHz reflected signal at the detector plane (solid line) folded with i) a high-gain antenna (dashed line) with an acceptance angle of 0.1 deg and ii) a low-gain antenna (dash-dotted line) with an acceptance angle of 21 deg. The location of the transmitter antenna is indicated with the solid bar at 0.5 m.

should have its own detector and that a waveguide run is needed from each of the receiver antennas to its detector.

An additional advantage of a poloidal receiver antenna array is that poloidal velocity measurements of the density turbulence can be made without much effort. By taking the cross correlation between the signals from two adjacent antennas the phase velocity of the scattered electrical field can be obtained. This velocity can then be related to the poloidal turbulent velocity via 2-D modeling. This technique was applied successfully on DIIID where a good agreement between poloidal velocities from charge exchange spectroscopy and poloidal correlation reflectometry was odtained [13].

In current reflectometer systems the transmitter and receiver antenna are often chosen to be identical. This might not be the optimal choice for a poloidal receiver antenna array on ITER. A strong reflected signal is obtained by keeping the ingoing beam as narrow as possible which means that the transmitter antenna should be a high gain antenna. With the receiver antennas one wants to collect the reflected radiation from a wide range of angles. This requires a low gain antenna as illustrated in fig. 8 where we have folded the reflected 190 GHz signal that was launched 10 cm below the plasma mid-plane with two different receiving antennas and calculated the antenna output as a function of the antenna location. The first receiver antenna had a high gain and hence a small acceptance angle of only 0.1 deg. and was alligned horizontally. This antenna only detects the small power near the launch antenna at 0.5 m but misses the strong reflection near 0.68 m due to its high directivity. The low-gain antenna on the other hand, with an acceptance angle of 21 deg., sees the strong reflected signal at 0.68 m. The width of both Gaussian receiver antennas was 9 cm. The transmitter antenna beam was the same as used previously: a 9 cm wide Gaussian beam without any spread.

The convex toroidal shape of the reflection layer spreads the reflected power in the toroidal direction and the received power will even be less than calculated here. Nevertheless, it is clear that only a low-gain wide-acceptance antenna is able to detect the reflected signal when it does not return back to the transmitter antenna.

VI. CONCLUSIONS

We have studied the response of the ITER low-field side reflectometer system where we have used the upper X-mode cut-off to probe a number of locations ranging from the low-field side edge to the halfway radius on the High-field side of the magnetic axis. For this study we have used a realistic 2-D ITER equilibrium with a constant electron density and a peaked electron temperature profile. As was found before [11] the reflection layer locations can shift by almost one meter compared to the cold-plasma approximation due to relativistic corrections. This shift has important consequences for low field side reflectometry on ITER as identified in this paper. The peaked electron temperature profile created concavely curved reflection layers near the plasma center. These concave reflection layers can form a focus for the reflected beam and create a smaller reflected beam at the detector plan than was

launched into the plasma. In the simulations it was also found that the reflected beam does not always return to the launch location. This is caused by a slight tilt of the reflection layers at the mid-plan due to ITERs highly asymmetric up-down plasma shape. In order not to miss the reflected signal under different ITER plasma scenarios, we propose to install a poloidal array of low-gain receiver antennas with a wide acceptance angle instead of a small number of transmitter-receiver antenna pairs. The transmitter antenna (or antennas) should be highly collimated for an optimal signal to noise ratio.

[1] G. Vayakis, T. Ando, N. Bretz, L. de Kock, A.J.H. Donné, E.J. Doyle, J. Irby, E. Martin, M. Manso, A. Mase, J. Sanchez, V.A. Vershkov, D. Wagner, C.I. Walker, and the ITER Joint Central Team and Home teams, Diagnostics for Experimental Thermonuclear Fusion Reactors 2, Edited by P.E. Stott, G. Gorini, P. Prandoni and E. Sindoni, Plenum Press, New York, 97 (1998).

[2] G. Vayakis private communication, 2005.

[3] E.J. Valeo, G.J. Kramer, and R. Nazikian, Plasma Phys. Contr. Fusion **44** L1 (2002).

[4] G.J. Kramer, R. Nazikian, and E.J. Valeo, Plasma Phys. Contr. Fusion **44** L11 (2002).

[5] G.J. Kramer, R. Nazikian, and E.J. Valeo, Rev. Sci. Instrum. **74** 1421 (2003).

[6] R. Nazikian, K. Shinohara, G.J. Kramer, E. Valeo, K. Hill, T.S. Hahm, G. Rewoldt, S. Ide, Y. Koide, Y. Oyama, H. Shirai, and W. Tang, Phys. Rev. Lett. 94, 135002 (2005)

[7] S.C. Jardin, N. Pomphrey, and J. DeLucia, J.Compt. Phys. **66** 481 (1983)

[8] J.E. Kinsey, G.M. Staebler, and R.E. Waltz, Phys. Plasmas **12** 052503 (2005).

[9] R.V. Budny, M.G. Bell, A.C. Janos, D.L. Jassby, L.C. Johnson, D.K. Mansfield, D.C. McCune, M.H. Redi, J.F. Schivell, G. Taylor, T.B. Terpstra, M.C. Zarnstorff, and S.J. Zweben, Nucl. Fusion **35**, 1497 (1995).

[10] D.B. Batchelor, R.C. Goldfinger, and H. Weitzner, Phys. Fluids **27** 2835 (1984).

[11] H. Bindslev, Plasma Phys. Contr. Fusion **34** 1601 (1992)

[12] H. Bindslev, Plasma Phys. Contr. Fusion **35** 1093 (1993)

[13] G.J. Kramer, T.L. Rhodes, W.M. Solomon, G.R. McKee, R. Nazikian, E. Valeo, R.V. Budny, and W.A. Peebles, 45th Annual Meeting of the American Physical Society Division of Plasma Physics, Albuquerque, New Mexico Oct. 27-31, GO1-14 130 (2003).

External Distribution

Plasma Research Laboratory, Australian National University, Australia

Professor I.R. Jones, Flinders University, Australia

Professor João Canalle, Instituto de Fisica DEQ/IF - UERJ, Brazil

Mr. Gerson O. Ludwig, Instituto Nacional de Pesquisas, Brazil

Dr. P.H. Sakanaka, Instituto Fisica, Brazil

The Librarian, Culham Science Center, England

Mrs. S.A. Hutchinson, JET Library, England

Professor M.N. Bussac, Ecole Polytechnique, France

Librarian, Max-Planck-Institut für Plasmaphysik, Germany

Jolan Moldvai, Reports Library, Hungarian Academy of Sciences, Central Research
    Institute for Physics, Hungary

Dr. P. Kaw, Institute for Plasma Research, India

Ms. P.J. Pathak, Librarian, Institute for Plasma Research, India

Dr. Pandji Triadyaksa, Fakultas MIPA Universitas Diponegoro, Indonesia

Professor Sami Cuperman, Plasma Physics Group, Tel Aviv University, Israel

Ms. Clelia De Palo, Associazione EURATOM-ENEA, Italy

Dr. G. Grosso, Instituto di Fisica del Plasma, Italy

Librarian, Naka Fusion Research Establishment, JAERI, Japan

Library, Laboratory for Complex Energy Processes, Institute for Advanced Study,
    Kyoto University, Japan

Research Information Center, National Institute for Fusion Science, Japan

Professor Toshitaka Idehara, Director, Research Center for Development of Far-Infrared Region,
    Fukui University, Japan

Dr. O. Mitarai, Kyushu Tokai University, Japan

Mr. Adefila Olumide, Ilorin, Kwara State, Nigeria

Dr. Jiangang Li, Institute of Plasma Physics, Chinese Academy of Sciences, People's Republic of China

Professor Yuping Huo, School of Physical Science and Technology, People's Republic of China

Library, Academia Sinica, Institute of Plasma Physics, People's Republic of China

Librarian, Institute of Physics, Chinese Academy of Sciences, People's Republic of China

Dr. S. Mirnov, TRINITI, Troitsk, Russian Federation, Russia

Dr. V.S. Strelkov, Kurchatov Institute, Russian Federation, Russia

Kazi Firoz, UPJS, Kosice, Slovakia

Professor Peter Lukac, Katedra Fyziky Plazmy MFF UK, Mlynska dolina F-2, Komenskeho Univerzita,
    SK-842 15 Bratislava, Slovakia

Dr. G.S. Lee, Korea Basic Science Institute, South Korea

Dr. Rasulkhozha S. Sharafiddinov, Theoretical Physics Division, Insitute of Nuclear Physics, Uzbekistan

Institute for Plasma Research, University of Maryland, USA

Librarian, Fusion Energy Division, Oak Ridge National Laboratory, USA

Librarian, Institute of Fusion Studies, University of Texas, USA

Librarian, Magnetic Fusion Program, Lawrence Livermore National Laboratory, USA

Library, General Atomics, USA

Plasma Physics Group, Fusion Energy Research Program, University of California at San Diego, USA

Plasma Physics Library, Columbia University, USA

Alkesh Punjabi, Center for Fusion Research and Training, Hampton University, USA

Dr. W.M. Stacey, Fusion Research Center, Georgia Institute of Technology, USA

Director, Research Division, OFES, Washington, D.C. 20585-1290